# POST-IRRADIATION EXAMINATION RESULTS FROM THE BTF-105A LOCA/LOECC TEST

VALLIANT, P.J., IRISH, J.D. and CRAIG, S.T.

Fuel Safety Branch
Reactor Safety Division
AECL, Chalk River Laboratories
Chalk River, Ontario, CANADA K0J 1J0

## ABSTRACT

The BTF-105A experiment was conducted in the Blowdown Test Facility of the NRU reactor. This CANDU-Owners-Group-sponsored test was part one of two simulations of the latter stages of a Loss-Of-Coolant Accident (LOCA) with additional Loss-Of-Emergency-Core-Cooling (LOECC). The BTF-105A test assembly consisted of an instrumented fuel stringer containing a single, unirradiated, fuel element. The primary objective of the BTF-105A test was to evaluate the instrumentation and procedures to be used in the BTF-105B test. This paper presents post-irradiation examination results from destructive examination of the BTF-105A fuel stringer in the hot cells at the Chalk River Laboratories.

## INTRODUCTION

The BTF-105A test [1] was conducted in the Blowdown Test Facility (BTF) of the NRU reactor (Figure 1). This CANDU-Owners-Group-(COG)-sponsored test was designed to evaluate the instrumentation and procedures to be used in the BTF-105B test and to determine the relationship between fuel-centreline and fuel-sheath temperatures under transient conditions with steam cooling. A single unirradiated fuel element was well instrumented with two fuel-centreline thermocouples, three sheath thermocouples attached by laser-welding and three high-temperature thermocouples attached to the sheath using Zircaloy clamps. Prior to the degraded-cooling transient, the test assembly was irradiated in pressurized water, at a linear power of approximately 50 kW/m for 10 days to establish an inventory of short-lived fission-products in the fuel element. Test conditions were representative of the degraded cooling environment during the latter stages of a Loss-Of-Coolant Accident (LOCA) with additional Loss-Of-Emergency-Core-Cooling (LOECC). After several hours of irradiation in saturated steam, the desired conditions were achieved by reducing the reactor power and depressurizing the test section. Following depressurization, the reactor power was increased in steps until fuel temperatures typical of those that would occur following a LOCA with additional LOECC were obtained. This also produced typical conditions for fission-product release and transport. At the peak of the transient, average fuel-centreline temperatures greater than 1900°C were maintained for about 5 minutes. The highly-oxidized fuel element failed when an unexpected quantity of

liquid condensate quenched the test section. The fission-product release was monitored and sampled by the BTF U-tubes and aerosol collectors after the fuel element failure. This paper presents post-irradiation examination results from destructive examination of the fuel stringer in the hot cells at the Chalk River Laboratories.

## BTF-105A FUEL ASSEMBLY

A cross section through the fuel element mid plane is shown in Figure 2. The single unirradiated fuel element was instrumented with two type-C fuel-centreline thermocouples (TFC01 and TFC02). The hot junction of TFC01 was located at the upper bearing pad elevation. TFC02 was located midway between the middle and bottom bearing pads. Three type-C, rhenium-clad thermocouples (TFS01, TFS02 and TFS03) were attached to the fuel sheath using Zircaloy clamps at the upper, middle and lower bearing pads (Figure 3). Three type-K, Zircaloy-clad thermocouples were laser welded to the fuel sheath (Figure 4) at the upper bearing pad (TFS06), midway between the upper and middle bearing pads (TFS04) and midway between the middle and bottom bearing pads (TFS05). The fuel element was contained within a coolant channel which was surrounded by a NILCRA (full density $ZrO_2$) insulator. The NILCRA was surrounded by a thermal shroud consisting of ZIRCAR (low density $ZrO_2$) insulation encased in a Zircaloy shell.

## POST-IRRADIATION EXAMINATION

The fuel assembly was gamma scanned in a storage can in the NRU reactor building after the test. The scan revealed a relatively intact fuel element (Figure 5). A decision was made to transfer the assembly to the hot cells without epoxying the assembly. This allowed much more information to be gained about instrumentation and the condition of the thermal shroud than would have been possible if the stringer had been epoxied initially. The ZIRCAR thermal insulation was cut longitudinally and the upper and lower halves were separated to expose the inner Zircaloy wall of the thermal shroud. In Figure 6 it can be seen that the inner Zircaloy wall is heavily oxidized and broken up at the elevation of the lower bearing pad of the fuel element. Evidence of steam ingress into the ZIRCAR insulation can be seen in the mating half of the thermal shroud where this ingress has discoloured the initially white ZIRCAR insulation. The insulation is mainly intact except for a through-wall crack that appears to line up with the zone of heaviest damage on the inner Zircaloy wall. It is possible, that the rapid injection of steam into the shroud following failure of the inner wall caused the through-wall crack in the insulation to form, which in turn, provided a path for the hot steam to heat the outer wall of the shroud directly. This would explain the rapid rise in temperature following shroud failure observed by a thermocouple located on the outside of the shroud [1]. This outer shroud thermocouple was located axially within a few millimetres of the observed crack in the insulation. A second gamma scan done in the hot cell showed some fuel relocation (Figure 5). A comparison of the two gamma scans indicates that most of the damage to the fuel element occurred during handling after the element was removed from the reactor. "Fuel powder"consisting of loose $UO_2$ fuel

particles, Zircaloy sheath pieces and $ZrO_2$ fragments from the thermal shroud were collected from the debris at the lower end of the fuel element for further analysis.

The fuel element and the NILCRA liner and Zircaloy tube of the thermal shroud were cast in epoxy. Transverse sections were taken at 5 elevations over the length of the fuel element, and the sections were examined metallographically (Figure 7). At each cross-section elevation, fuel-sheath-oxide thicknesses were measured along with $UO_2$ grain size at the centre, mid radius and periphery of the fuel (Table 1). The $UO_2$ grain size has remained relatively unchanged from as fabricated due to the low temperature (fuel-centreline temperature ~1400°C) during the 10-day irradiation in pressurized water and due to the short time that the fuel element was at high temperature during the transient. Sheath oxidation ranged from minimal at the top of the fuel element (Figure 8) to through-wall oxidation over the whole bottom half of the fuel element (Figure 9). The $UO_2$ fuel was heavily cracked throughout the fuel element with fuel relocation in the lower elevations. Figure 10 illustrates the totally oxidized sheath at the lower element elevation. The lower bearing pad (Figure 11) shows the extent of oxidation and sheath transformation. Near the end of the transient, liquid water passed through the test section. At this time the temperature indicated by TFS03 dropped 1200°C in 10 seconds. The thermal shock from this quench resulted in a shattered appearance of the fuel, sheathing and NILCRA insulation at the lower elevations (Figure 9). It has been hypothesized [2] that this quench contributed to fuel sheath failure. Metallography at various elevations showed the rhenium clad thermocouples remained intact, confirming that they survived the transient in reasonable mechanical condition. Figure 8 shows the fuel-centreline thermocouple, TFC01, and external sheath thermocouples, TFS01 and TFS02, from the upper bearing pad location. They appear to be mechanically sound with no apparent sign of damage. TFS03, seen in Figure 9, remains intact and is surrounded by relocated fuel sheathing and $UO_2$ fuel. The good performance of thermocouples TFS02 and TFS03 [1] attached with Zircaloy clamps, together with the good mechanical condition of the thermocouples as indicated by PIE, showed that thermocouples of this type and the method of attachment should be used for future BTF tests.

Interaction of $UO_2$ and the Zircaloy-4 fuel sheath is shown in Figure 12. This sample was from the lower bearing pad region. The interaction may have been facilitated by the close contact between the fuel and sheath at the Zircaloy clamp area [3]. It appears as though an $\alpha$-Zr(O) + U(Zr) layer has formed at the interface between the fuel and sheath. The sheath has been oxidized by oxygen which has diffused out of the fuel.

The powdering of the $UO_2$ near the bottom of the fuel element could have been caused by the thermal quench. However, the fuel powdering could also be due to $UO_2$/Zr interaction. Figure 13 shows a SEM photo of a $UO_2$ grain. Analysis indicates that the grain contains U and Zr. It is possible that there are some zirconia fragments on the surface of the grain since the powder is a mixture of material from the fuel element and the shroud. The small white particles which are imbedded in the grain are very similar to the "flowers" of $UO_2$ observed by Evans et al. [4] when excess U (due to the $UO_2$/Zr interaction) which had deposited on the grain boundary was oxidized by steam. The fuel temperatures of 300-500°C for the 5 minutes immediately following the quench are just those identified by Evans as most likely to lead to fuel fragmentation following U/Zr interaction. An SEM of the powder, Figure 14, shows the presence of $UO_2$ fuel

and a Zircaloy droplet indicating that high temperatures in the vicinity of 1760-1950°C, the melting range of partially oxygenated Zircaloy, were attained.

Aerosol collector tray liners were also examined using SEM. The top tray liner identified as A1 (Figure 15) captured the large particles. These particles were mainly stainless steel and a copper/calcium combination likely from contaminants in the system arising from cutting, and welding operations, and thread lubricants. The bottom tray liner identified as A12 (Figure 16) contained a fine particulate (including Zr, Cu, Be, Fe, Cr, Si, etc.). With the exception of Zr and Be, these are all structural materials which are not associated with the fuel element. Gamma scans were consistent with the SEM results in the sense that only trace amounts of fission products were detected. However, the gamma scans were done several months after the test, therefore the short- and intermediate-half-life fission-products could have decayed beyond detection. When examined by SEM, blowdown tank coupons taken from the liquid portion of the tank generally had more material deposited on them than did coupons from the vapour portion of the tank. The observed elements were similar to those found on the aerosol collector trays.

## CONCLUSIONS

One of the main objectives of the BTF-105A test was to investigate instrumentation improvements for the BTF-105B test. Good performance of the fuel-centreline and the high-temperature fuel-sheath thermocouples was seen in the BTF-105A test. The high-temperature rhenium-clad thermocouples attached with Zircaloy clamps remained operational and PIE showed them to be in good mechanical condition after the test. As a result, this technology was used for the BTF-105B test.

It appears that following the failure of the inner Zircaloy wall of the thermal shroud, a jet of steam may have impinged on the ZIRCAR insulation causing a large crack in the insulation which allowed the steam to impinge on the outer Zircaloy wall of the shroud causing the outer shroud temperature to increase rapidly.

Evidence of $UO_2$/Zr interaction was found. This likely contributed to the breakup of some of the fuel into grain-size pieces.

Data obtained from $UO_2$ grain growth measurements and sheath oxide thicknesses are available for the validation of computer codes used in the safety analysis and licensing of CANDU reactors.

## ACKNOWLEDGEMENTS

The authors acknowledge the financial support of the CANDU Owners Group, consisting of the Canadian nuclear utilities (Ontario Power Generation, Hydro-Québec and New Brunswick

Power) and AECL. The authors would also like to acknowledge the contribution of J.W. DeVaal who was the BTF-105A test director and guided much of the BTF-105A PIE.

REFERENCES

1. DEVAAL, J.W. et al., "Preliminary Results of the BTF-105A Test: An In-Reactor Instrument Development and Fuel Behaviour Test", Proceedings of the Canadian Nuclear Society: Fifth International Conference on CANDU Fuel, Toronto, 1997 September 21-25.

2. ARIMESCU, V.I., "Quench Features of the BTF-105A Experiment: Preliminary Data and Modelling", Presentation to Fourth International QUENCH Workshop, Forschungszentrum Karlsruhe, 1998 October 6-8.

3. DIENST,W., HOFFMAN, P. and KERWIN-PECK, D.K., "Chemical Interactions Between $UO_2$ and Zircaloy-4 from 1000 to 2000°C," Nucl. Technol. 65(1984) 109.

4. EVANS, D.G. et al., "Effect of the $UO_2$ / ZR Interaction on the Fragmentation of Unirradiated $UO_2$ Fuel Pellets", Proceedings of the Canadian Nuclear Society: Twelveth Annual Conference, Saskatoon, 1991 June 9-12.

**TABLE 1: GRAIN SIZE MEASUREMENTS**

| Met Identity | Location | Measurement 1 | Measurement 2 | Measurement 3 | Average Size (μm) | Met Location |
|---|---|---|---|---|---|---|
| II27B | Periphery | 7.1 | 7.1 | 7.4 | 7.2 | Met 1 Side B |
| | Mid-Radius | 7.4 | 7.1 | 7.4 | 7.3 | " |
| | Center | no boundaries on grains, possibly fuel here is $U_3O_8$ | | | | |
| II27D | Periphery * | 8.0 | 8.3 | 9.5 | 8.6 | Met 3 Side D |
| | Mid-Radius** | 6.9 | 6.7 | 7.1 | 6.9 | " |
| | Center*** | n/a | | | | |
| II27F | Periphery | 8.7 | 9.1 | 11.1 | 9.6 | Met 4, Side F |
| | Mid-Radius | 7.7 | 6.9 | 8.0 | 7.5 | " |
| | Center | 8.3 | 8.0 | 8.7 | 8.3 | " |
| II27 G | | all the fuel fragments had small grains which are often found at the periphery or mid-radius of the pellet; none of the fragments had larger grains; the measurements that follow are random measurements found in different fragments | | | | |
| | Random Fragments | 10.5 | 8.7 | 8.0 | 9.1 | Met 4 Side G |

*fuel fragment was selected because morphology of piece resembles a periphery piece,

**fuel fragment was selected because radial crack in sample resembles that often found near mid-radius.

***all fragments contained smaller axial grains, no larger/columnar grains often associated with grains in the center of the pellet were noted.

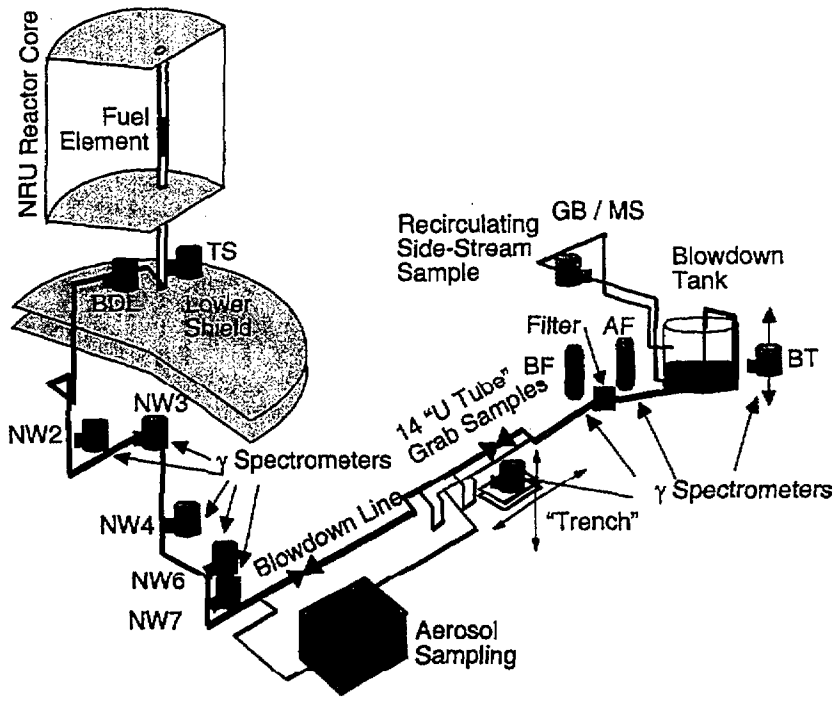


Figure 1: Schematic Drawing of the Blowdown Test Facility

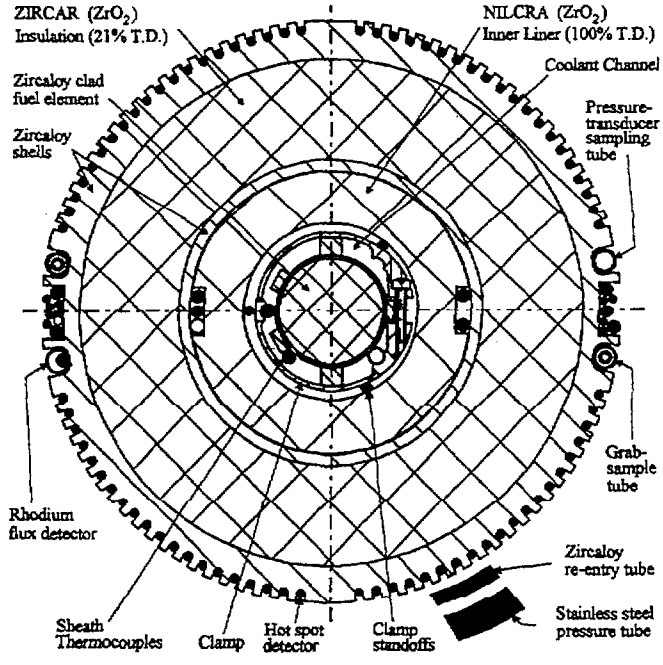


Figure 2: Cross Section Through the BTF-105A Test Assembly at the Fuel Element Midplane

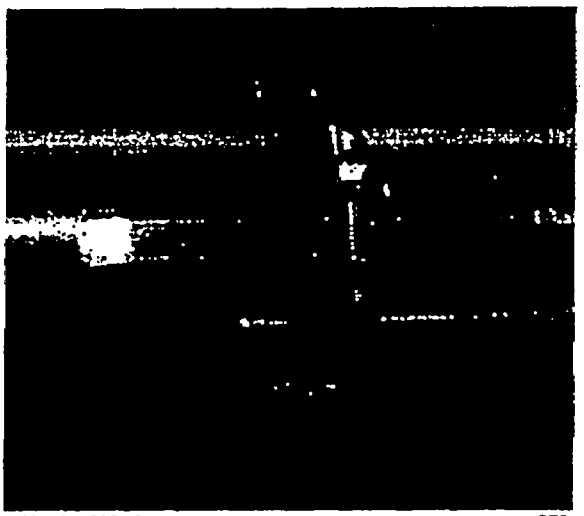

9601-22613-6 3X

Figure 3: Zircaloy Clamp at Lower Bearing Pad Securing Type-C Rhenium Clad Thermocouples to Sheath

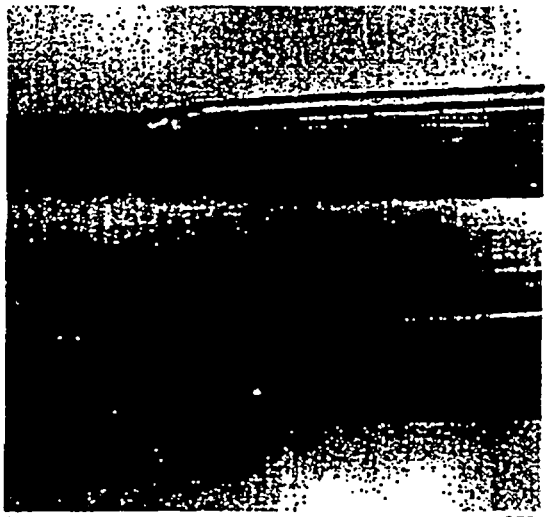

9602-22630-4 3X

Figure 4: Type-K Zircaloy Clad Thermocouple Laser Welded to Sheath Located Midway Between Middle and Lower Pads

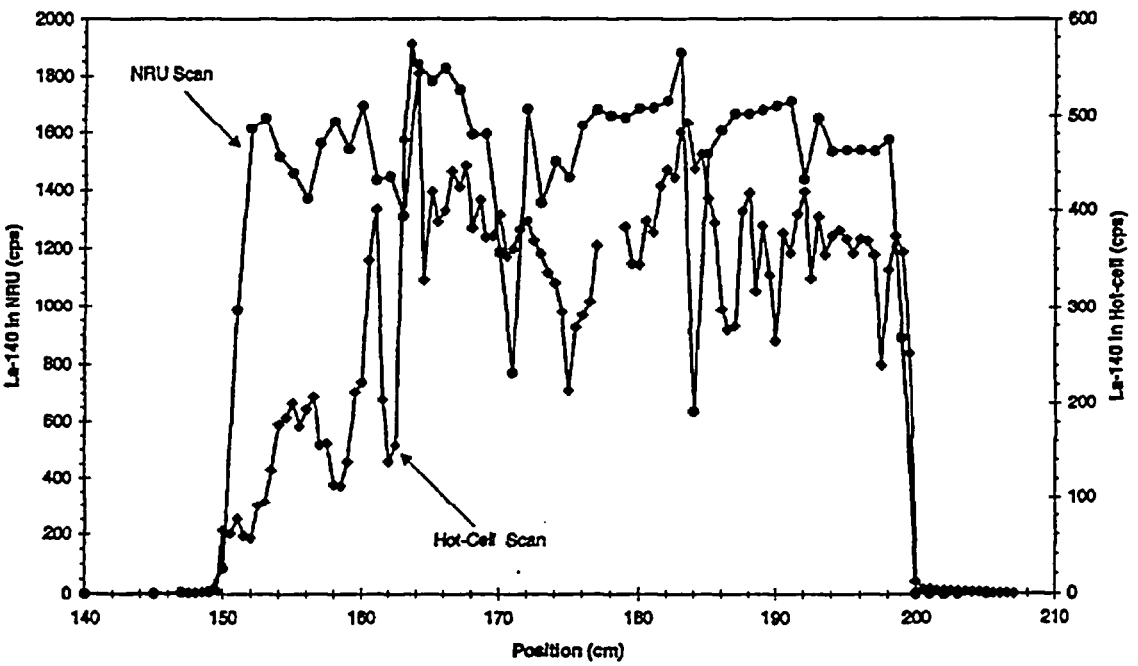


Figure 5: Comparison of La-140 Gamma Scans Performed in the NRU Storage Block and in the Hot Cells

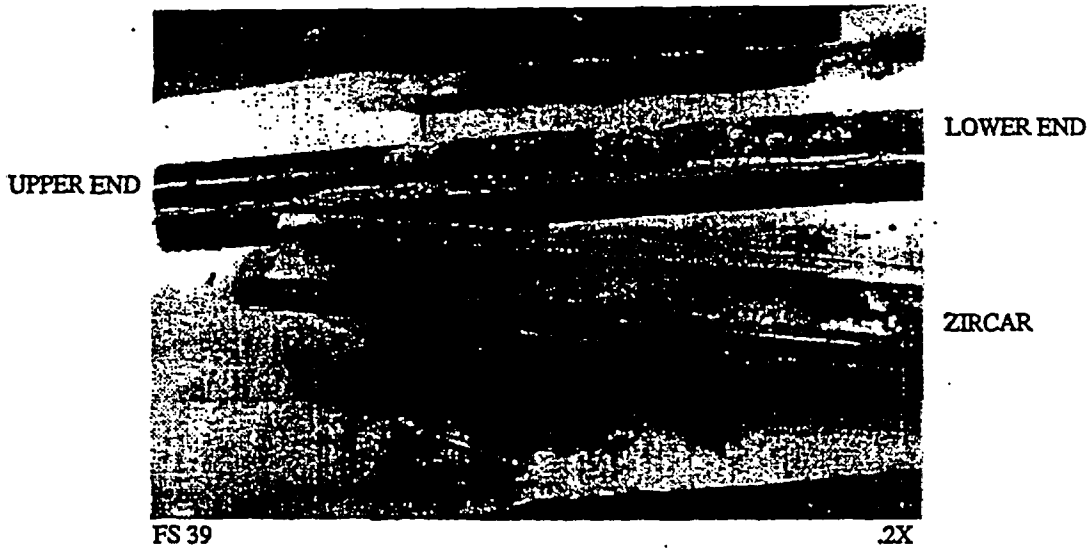


Figure 6: BTF-105A Fuel Assembly and ZIRCAR Liner

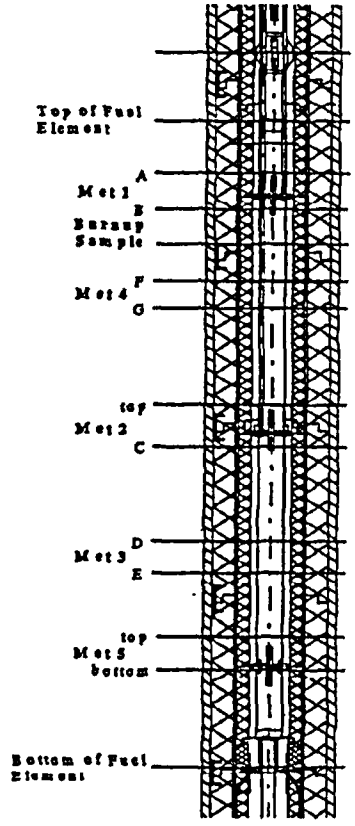


Figure 7: BTF-105A Post-Irradiation Examination Sections

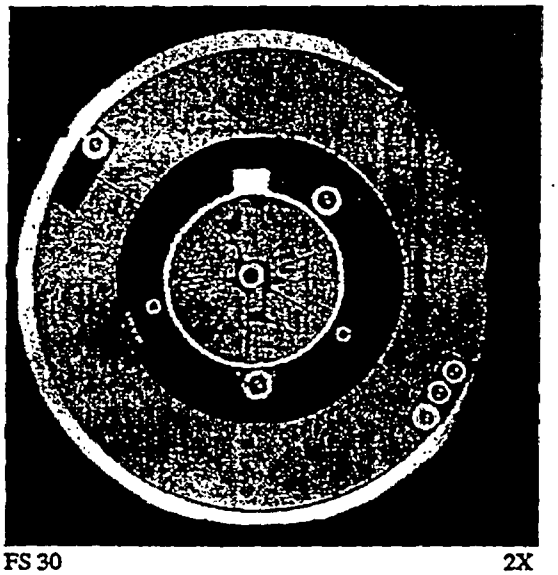

FS 30 2X

Figure 8: Met 1 Upper Bearing Pad - TFC01

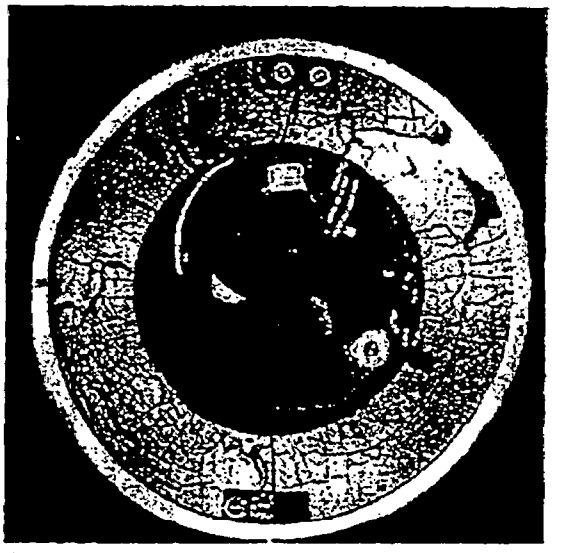

FS 25 2X

Figure 9: Met 2 Middle Bearing Pad

JJ 7D2 5.2X

Figure 10: Met 3 Fully Oxidized Sheath

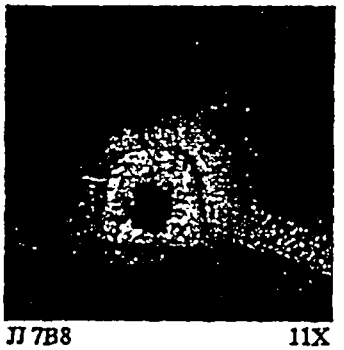

JJ 7B8 11X

Figure 11: Oxidized Condition of Lower Bearing Pad

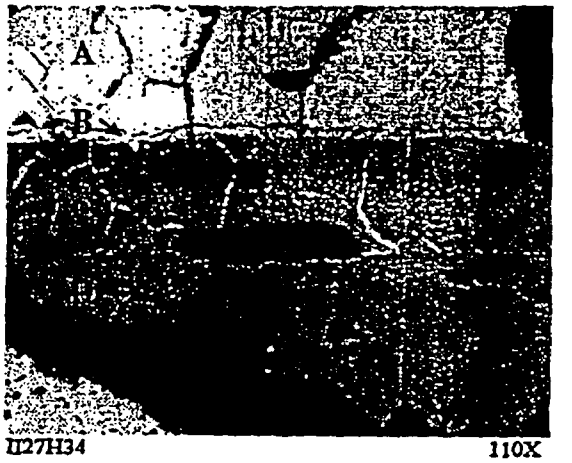


JJ27H34 110X

A - α - Zr(O)
B - U(Zr)
C - α - Zr(O) + U(Zr)
D - $UO_2$ Fuel

Figure 12: Interaction of $UO_2$ and Zr-4 Fuel Sheath at Lower Bearing Pad


4000X

Figure 13: SEM Photo of $UO_2$ Grain with Small Particles Present, Possibly Imbedded

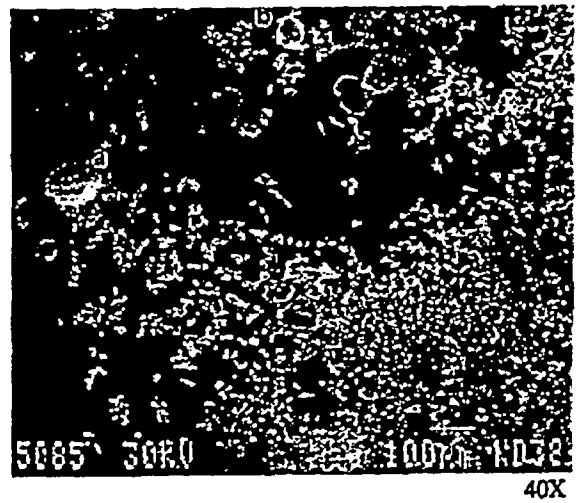


40X

Figure 14: SEM Photo Reveals Presence of $UO_2$ Fuel (a) and Zircaloy Droplet (b)

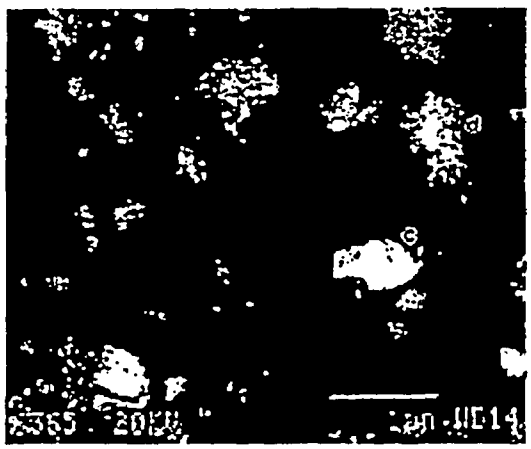


16X

Figure 15: SEM Photo Displays Large Particles from Top Tray Liner (A1) of Aerosol Canister. Stainless Steel (c) and Copper/Calcium (d) Particles are Shown

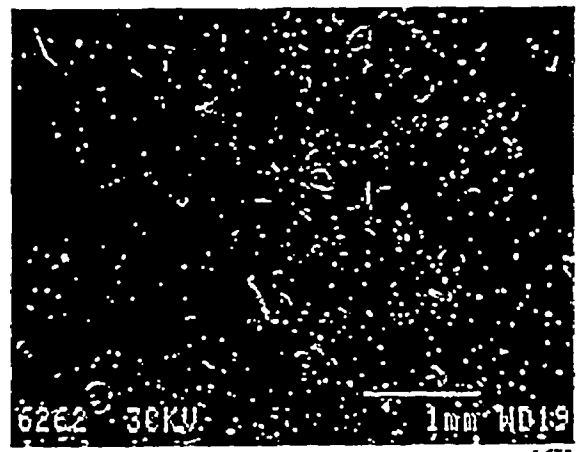


16X

Figure 16: SEM Photo Displays Small Particles from Bottom Tray Liner (A12) of Aerosol Canister. Silicon, Chromium, Iron, and Stainless Steel Particles Present